Virology **266,** 79–87 (2000)
doi:10.1006/viro.1999.0071, available online at http://www.idealibrary.com on IDEAL®

Genetic Dissection of Tomato Bushy Stunt Virus p19-Protein-Mediated Host-Dependent Symptom Induction and Systemic Invasion

Meihua Chu,[1] Bénédicte Desvoyes, Massimo Turina,[2] Robert Noad,[3] and Herman B. Scholthof[4]

Department of Plant Pathology and Microbiology, Texas A&M University, College Station, Texas 77843

Received April 28, 1999; returned to author for revision June 3, 1999; accepted October 27, 1999

The plus-sense single-stranded RNA of tomato bushy stunt virus (TBSV) encodes a 19-kDa protein, which is translated from a 3′ proximal open reading frame (p19) that is entirely nested within the cell-to-cell movement gene (p22). Expression of the cytosolic p19-protein induces either a systemic lethal collapse in *Nicotiana benthamiana* and *N. clevelandii,* or necrotic local lesions on resistant *N. tabacum.* In spinach, the p19-protein is required at high abundance for efficient systemic invasion. This study aimed to determine whether these seemingly different host-dependent biological activities are governed by the same or separate regions on the 172 amino acid p19-protein. For this purpose, codons for charged amino acids predicted to be exposed on the surface of the polypeptide and presumably available for host-specific interactions, were targeted for mutagenesis. A total of 12 mutants were generated, which had no deficiencies in replication or cell-to-cell movement, and substitution of amino acids at the extreme N-terminal end or within the carboxyl 70 amino acids failed to cause a noticeable biological effect on plants. However, mutations dispersed between positions 43 and 85 on the N-terminal half prevented the onset of a systemic lethal necrosis on *N. benthamiana* and *N. clevelandii.* With one exception, the same mutants elicited mostly chlorotic, rather than necrotic, local lesions on *N. tabacum.* Mutations in the central region, which substituted Arg with Gly at positions 72 or 75–78, impaired the ability of TBSV to systemically invade spinach plants. However, substitution with Ala instead of Gly at position 72 had minimal effects on systemic spread in spinach, suggesting the possible influence of protein structure effects. The implications are that regions on the N-terminal portion of the p19-protein mediate interactions in a host-dependent manner and that a central region is required for all activities either by a direct effect of the amino acids or through maintenance of structural integrity.

INTRODUCTION

While many plant viruses may replicate in single cells of numerous plant species, and perhaps even move from cell-to-cell, the host range of a plant virus is predominantly determined by its ability to systemically invade the whole plant. However, even when initial virus movement occurs, some resistant plants can specifically recognize individual virus-encoded products to activate a hypersensitive response (HR) around the site of infection to prevent further spread of the virus. When resistance responses are not activated, a systemic infection can occur to result in symptoms that may range from very mild to lethal.

Tomato bushy stunt virus (TBSV) accumulates to high titers in a variety of plants and the host-range includes more than 100 plant species in 20 families of mono- and dicotyledonous plants (Martelli *et al.,* 1988; Russo *et al.,* 1994). TBSV particles contain a positive-sense single-stranded RNA genome of 4775 nucleotides (nt), with five major open reading frames (ORFs) (Hearne *et al.,* 1990), as shown in Fig. 1. The genomic RNA functions as an mRNA for the translation of two 5′ proximal genes, p33 and the read-through p92 ORF, which are both required for replication (Scholthof *et al.,* 1995c). During replication, two subgenomic RNAs (sgRNAs) are produced via a mechanism that involves core promoters and distal RNA segments (Johnston and Rochon, 1995; Zhang *et al.,* 1999). The sgRNA1 transcripts are used for translation of the internal 41-kDa coat protein gene (p41), and two small nested genes located near the 3′ terminus of tombusvirus genomes are translated from sgRNA2 (Fig. 1) (Hayes *et al.,* 1988; Hearne *et al.,* 1990; Hillman *et al.,* 1989; Johnston and Rochon, 1996). For TBSV, these p22 and p19 genes yield a membrane bound cell-to-cell movement protein of 22 kDa, and a cytoplasmic protein of 19 kDa, respectively (Scholthof *et al.,* 1995b).

TBSV and its p19 gene provide a suitable genetic model system to investigate the differences and similarities between virus–host interactions in susceptible versus resistant plants. For example, the p19-protein mediates three phenotypically distinct activities: it is required for systemic spread of TBSV in some hosts (e.g., spinach) (Scholthof *et al.,* 1995b), it activates a hypersensitive

[1] Current address: Hitachi Software, 601 Gateway Blvd. Suite 500, South San Francisco, CA 94080-7025.
[2] Current address: Department of Plant Pathology, University of California, Davis, CA 95616.
[3] Current address: Department of Biochemistry, University of Oxford, South Parks Road, Oxford, OX1 3QU, UK.
[4] To whom correspondence and reprint requests should be addressed. Fax: (409) 845-6483. E-mail: herscho@acs.tamu.edu.

0042-6822/00 $35.00

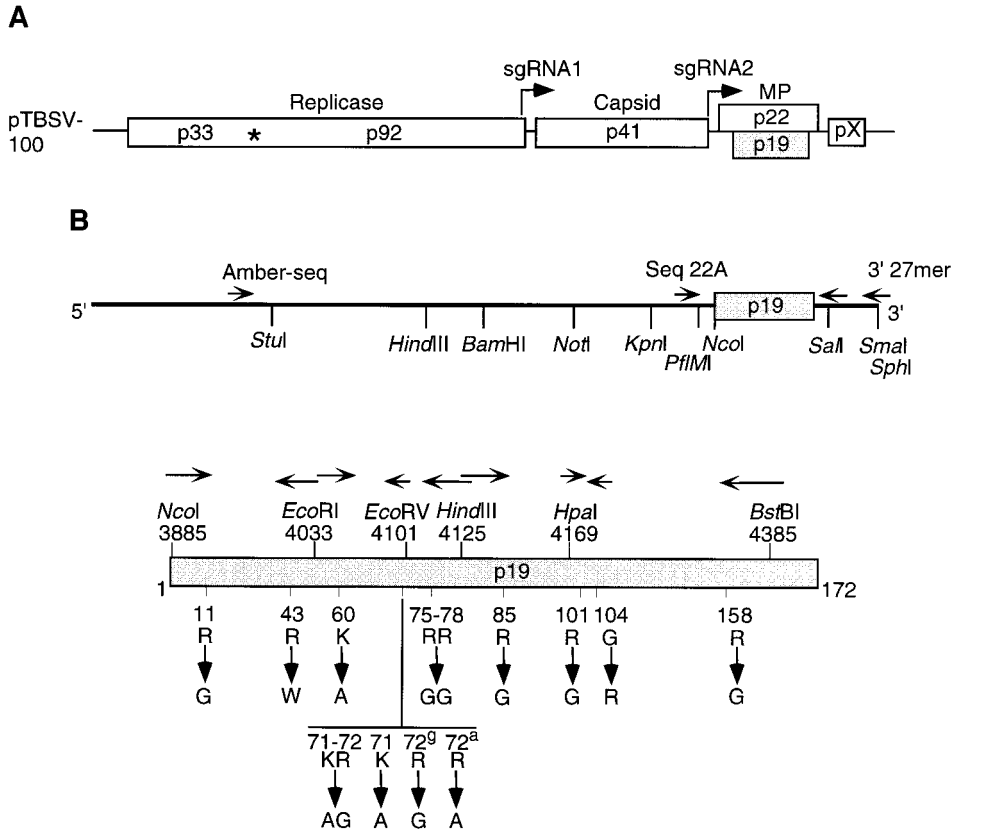

FIG. 1. Schematic diagram of the TBSV genomic organization and the derived p19 mutants. (A) Open boxes denote open reading frames (ORFs) that encode proteins for which sizes are given in kDa inside the boxes, and the functions are indicated on top. MP indicates movement proteins. The function of the putative pX product is unknown. Solid lines represent presumed untranslated sequences, and the transcriptional start-sites of subgenomic RNAs (sgRNA1 and sgRNA2) are indicated by right-angled arrows. The asterisk inside the TBSV genome indicates the relative position of the amber stop codon used for translational read-through of p33 to yield the p92 product. (B) The polarity and location of primers on the whole genome outside the p19 gene (top) and within the p19 gene (bottom). The arrows display the primers in the 5′ to 3′ direction, and nucleotide positions of restriction enzyme sites are provided. The position of the target amino acids is indicated and the substitutions are denoted by the conventional single-letter notation along the polypeptide of 172 aa.

response-like (HR-like) reaction in selected resistant plant species (e.g., *Nicotiana tabacum*), whereas in the susceptible hosts *N. benthamiana* and *N. clevelandii* the p19-protein induces a systemic lethal collapse (Scholthof *et al.,* 1995a). The objective of this study was to determine whether identical or separate domains on the p19-protein are involved in these three, seemingly different host-specific biological activities.

This investigation focused mainly on charged amino acids that were considered candidates for exposure on the p19-protein surface and therefore potentially involved in host-specific interactions. Codons for individual or clustered residues were targeted for mutagenesis, while avoiding the introduction of changes in the overlapping p22 ORF. The results showed that substitutions of amino acids in the N-terminal portion of the p19-protein affected induction of systemic and local symptoms in the *Nicotiana* hosts without impairing virus spread in spinach, while a central region of the p19-protein was shown to be essential for all three tested biological activities.

RESULTS

Characteristics of mutant p19-proteins

To evaluate the contribution of presumably surface-exposed p19-protein residues to the various biological activities, clustered or individual charged amino acids were targeted for mutagenesis. The feature that the p19 gene is completely nested within the p22 gene (Fig. 1) limited not only the number of nucleotides that were available for mutagenesis without disturbing p22, but also the choice of substitute amino acids. Within these limitations, 11 p19 mutants were generated by changing codons for charged amino acids to codons for neutral residues (Fig. 1). A 12th mutant (pT19/104) produces a p19-protein in which a hydrophilic amino acid (R) replaces a glycine residue (G) (Fig. 1). The mutants are designated using the notation pT19/a_n, which indicates that the plasmid (p) containing the full-length cDNA of TBSV (T) is mutated in the p19 gene (19) at the indicated codon (i.e., amino acid) position(s) given by "a" ("n" indi-

TABLE 1

Oligonucleotide Primers Used for Site-Directed Mutagenesis of the TBSV p19 Gene

aa[a]	Oligonucleotide,[b] 5′ to 3′	Position[c]	R.e.
11	AA ACC ATG GAA CGA GCT ATA CAA GGA AAC GAC GCT gGG G	3882–3920 (F)	*Nco*I
43	G TGG tGG CTA CAT AAC GAT GAG ACG AAT TCG AAT C	4043–4009 (R)	*Eco*RI
60	G ACG AAT TCG AAT CAA GAT AAT CCC CTT GGT TTC gcG GAA AG	4030–4071 (F)	*Eco*RI
71	T GTA TTT gcG AGA TAT CTC AG	4110–4090 (R)	*Eco*RV
72[a]	GTT GTA TTT AAG gct TAT CTC AGA TAC GAC	4117–4088 (R)	—
72[g]	T GTA TTT AAG gGA TAT CTC AG	4110–4090 (R)	*Eco*RV
71–72	T GTA TTT gcG gGA TAT CTC AG	4110–4090 (R)	*Eco*RV
75–78	AT CTC gGA TAC GAC gGG ACG GAA GCT TCA C	4133–4104 (R)	*Hin*dIII
85	CG GAA GCT TCA CTG CAC gGA GTC	4122–4144 (F)	*Hin*dIII
101	TCG GTT AAC TAT GCA GCA TCT gGA TTT T	4166–4193 (F)	*Hpa*I
104	TCT CGA TTT TTC cG T TTC GAC CAG	4207–4184 (R)	—
158	GTA TCA gGA GGA TGC CCT GAA GGT ACT GAG ACC TTC GAA AAA	4393–4352 (R)	*Bst*BI

[a] Amino acid (aa) position on the p19-protein affected by the mutation(s).

[b] Although reverse primers (R) (see Fig. 1 and third column in table) were composed of minus-sense sequences, for purposes of clarity the sequence is given in the positive-sense orientation and nucleotides are grouped as triplets for the p19 ORF. The lowercase letters represent the mutated nucleotides; restriction endonuclease sites in primers that were used to transfer fragments are underlined and the corresponding restriction enzymes (R.e.) are shown in the righthand column; the minus (−) sign indicates that primers were employed for mutagenesis on single-stranded DNA (Materials and Methods).

[c] Nucleotide position of the primers and the forward (F) or reverse (R) orientation of the primers, which is also indicated in Fig. 1.

cates that some constructs have more than one codon changed; absence of the notation "p" refers to RNA). Table 1 shows the sequence and other relevant features of the primers used to generate the site-specific p19 mutants.

The RNA accumulation of the mutants was assayed in *N. benthamiana* protoplasts in several experiments; an example of results is provided in Fig. 2. Comparison of gRNA yield with the amount of rRNA, combined with RNA hybridization assays, consistently showed that the accumulation of viral RNA and ratio of gRNA versus sgRNAs is comparable for all mutants and wild-type. Although the intensity of signals was sometimes variable between samples, these variations were not consistent between experiments, and lower amounts of gRNA correlated with lower amounts of rRNA (e.g., T19/71–72 and T19/75–78 in Fig. 2) or with reduced levels of input transcripts (e.g.,

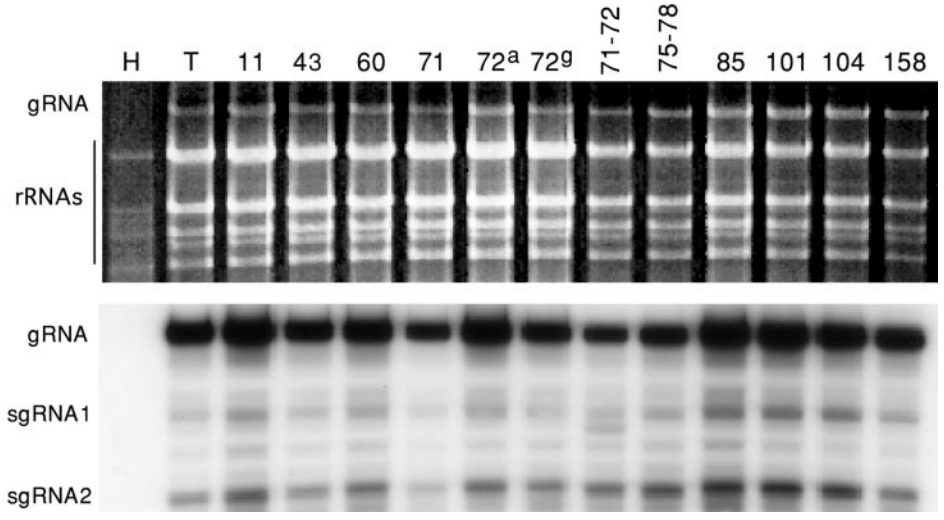

FIG. 2. RNA accumulation in *N. benthamiana* protoplasts transfected with TBSV p19 mutants, as inferred by (A) intensity of gRNA compared to rRNA on an EtBr stained agarose gel, and (B) subsequent hybridization to a TBSV-specific probe. The numerical designation of the constructs corresponding to those in Fig. 1 is provided above each lane, and H represents RNA from healthy mock inoculated protoplasts. The position of genomic RNA (gRNA) and the two subgenomic RNAs (sgRNA1 and sgRNA2) are indicated. Random primed pHS54 (Scholthof *et al.,* 1993a) was used as the hybridization probe. The origin of the enhanced shadow band underneath sgRNA1 for T19/71–72 is not known; its appearance was not consistent.

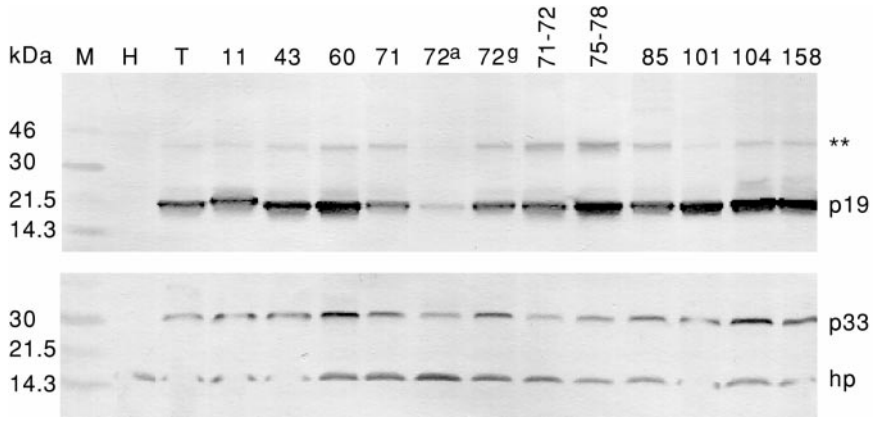

FIG. 3. Immunodetection of TBSV proteins in inoculated leaves of *N. benthamiana*. Leaves were harvested 5 days postinoculation with transcripts. Standard alkaline-phosphatase-mediated reactions were employed for immunodetection of the p19-protein (upper panel) or the p33-protein (lower panel). The double asterisks indicate the position of presumably dimeric forms of the p19-protein. An unknown host protein (hp) cross-reacted with the p33 antiserum. A sample from healthy plants (H) was used as a control, and the molecular weight of size markers (M) in kDa is provided on the left.

T19/71 in Fig. 2). Therefore, our cumulative results did not detect an effect of the p19 mutations on TBSV RNA accumulation.

Inoculations of *N. benthamiana* leaves with the mutants showed that they were competent for cell-to-cell movement as inferred by the appearance of localized symptoms (data not shown). The accumulation of the p33-protein correlates with the amount of TBSV RNA (Scholthof *et al.,* 1999), and the accumulation of p33-protein and p19-protein was similar for the mutants and wild-type TBSV 5 days postinoculation of *N. benthamiana* (Fig. 3). In the experiment shown in Fig. 3, for unknown reasons the accumulation of p19-protein, but not the p33-protein, appears reduced in leaves inoculated with RNA from pT19/71 and pT19/72^{a}, compared to wild-type. However, because those mutations had no abnormal effects on subsequent biological tests (discussed later), this was not further investigated. Furthermore, the mutant RNAs from pT19/72^{g}, pT19/71–72, pT19/75–78, and pT19/85, which display the most prominent effects on all three biological activities tested in whole plants (see later discussion), accumulate to similar levels as wild-type TBSV.

Infections of *N. benthamiana* or spinach with RNA from pT19/11 consistently yielded a p19-protein that upon SDS–PAGE migrated slightly slower than all the other p19-proteins (Fig. 3). However, no obvious biological effects were noticed. Sequence analysis of the entire p19 gene of pT19/11 eliminated the possibility that the change in protein migration was due to serendipitous alterations because only the intended mutation was present.

Effects of p19 mutations on systemic symptoms in *N. benthamiana* and *N. clevelandii*

The p19-protein of TBSV, or its analog of other tombusviruses, is dispensable for systemic infection of *N. benthamiana* and *N. clevelandii* but affects the symptom phenotype (Dalmay *et al.,* 1993; Reade *et al.,* 1999; Rochon, 1991; Scholthof *et al.,* 1995a). For example, the apical necrosis and subsequent death upon infection of plants with TBSV, is a result of p19-protein expression (Scholthof *et al.,* 1995a), although other factors may contribute (Havelda *et al.,* 1998). To evaluate the contribution of distinct p19-protein domains to this severe symptom phenotype, the p19 mutants were inoculated onto *N. benthamiana* and *N. clevelandii*, and the combined results are summarized in Table 2. The data show that mutations of amino acids between positions 43 and 78 interfered with the induction of a systemic collapse. Although the mutations in T19/75–78 prevented the onset of necrosis, mutants with substitutions between positions 43 and 72 retained the ability to induce necrosis on lower leaves. Emerging leaves of plants infected with these mutants displayed typical vein clearing and mosaic symptoms, but these did not progress into a systemic collapse.

Effects of p19 mutations on elicitation of necrotic local lesions on *N. tabacum*

The p19-protein of TBSV is responsible for the elicitation of small necrotic local lesions on *N. tabacum*, which effectively arrest the spread of the virus (Scholthof *et al.,* 1995a). To determine which p19-protein residues are critical for elicitation of this HR-like response, the p19 mutants (Fig. 1) were inoculated onto *N. tabacum*, and the results are summarized in Table 2. Except for the mutation in pT19/60, all the mutations introduced between positions 43 and 85 elicited a different local lesion response than wild-type. Light and temperature conditions influenced the lesion phenotype, but the lesions induced by the aforementioned mutants were mostly chlorotic, similar to that observed for the mutant pHS157,

TABLE 2

Summarized Effects of p19 Mutation on Host-Specific Responses

Construct	Amino acid	*N. benthamiana* *N. clevelandii* [a]	*N. tabacum* [b]	Spinach [c]
pTBSV	WT	+++	+	+++
pT19/11	R11G	+++	+	+++
pT19/43	R43W	+	−	+++
pT19/60	K60A	+	+	+++
pT19/71	K71A	+	−	+++
pT19/72[a]	R27A	+	−	+++
pT19/72[g]	R72G	+	−	−
pT19/71–72	KR71–72AG	−	−	−
pT19/75–78	RR75–78GG	−	−	+
pT19/85	R85G	++	−	++
pT19/101	R101G	+++	+	+++
pT19/104	G104R	+++	+	+++
pT19/158	R158G	+++	+	+++

Note. Original amino acids are depicted on the left of the numbered positions on the p19 polypeptide (172 amino acids), and the substitute residues are provided on the right of the number. WT indicates the wild-type p19-protein.

[a] Effects of the mutation on the p19-mediated systemic lethal necrosis phenotype. Three plus signs (+++) represent the total lethal necrosis typically observed upon infection with wild-type TBSV. A single plus sign (+) denotes that lower leaves still become necrotic but a systemic collapse fails to occur. A minus sign (−) indicates absence of, or recovery from, necrotic symptoms, and (++) indicates minimal effects.

[b] The necrotic local lesion response typical for wild-type is indicated by a plus sign (+), whereas a minus sign (−) denotes the absence of local lesions typically elicited by wild-type virus.

[c] Triple plus signs (+++) indicate effective systemic invasion of spinach whereas a minus sign (−) illustrates the absence of long distance spread. A single plus sign (+) is indicative of a noticeable delay in infection by 4–6 days, and ++ indicates only a slight delay of 2–3 days.

which is inactive for p19 expression (Scholthof *et al.,* 1995b).

Effects of p19 mutations on systemic invasion of spinach

The p19 mutations upstream from amino acid position 71 or downstream from position 85 did not noticeably affect the ability of TBSV to systemically invade spinach plants (Table 2). Compared to wild-type TBSV, the onset of systemic symptoms on spinach by T19/85 or T19/75–78 was delayed by 2–3 or 4–6 days, respectively. This difference was confirmed by immunoblot analyses, which showed that 10 days postinoculation T19/85 was present in low amounts in upper noninoculated leaves but T19/75–78 was not yet detectable (Fig. 4A). These results demonstrate that the rate of TBSV spread through spinach was affected slightly by the mutation of pT19/85 and more substantially by the changes in pT19/75–78. The mutant T19/71–72 caused the onset of local necrotic lesions on inoculated spinach leaves, but consistently failed to systemically invade these plants, as confirmed by Western assays (Figs. 4A and 4B). Only when very young plants were inoculated did some scattered systemic symptoms occur (data not shown).

To separate the contribution of the Lys to Ala change at position 71 from the effect due to the Arg to Gly change

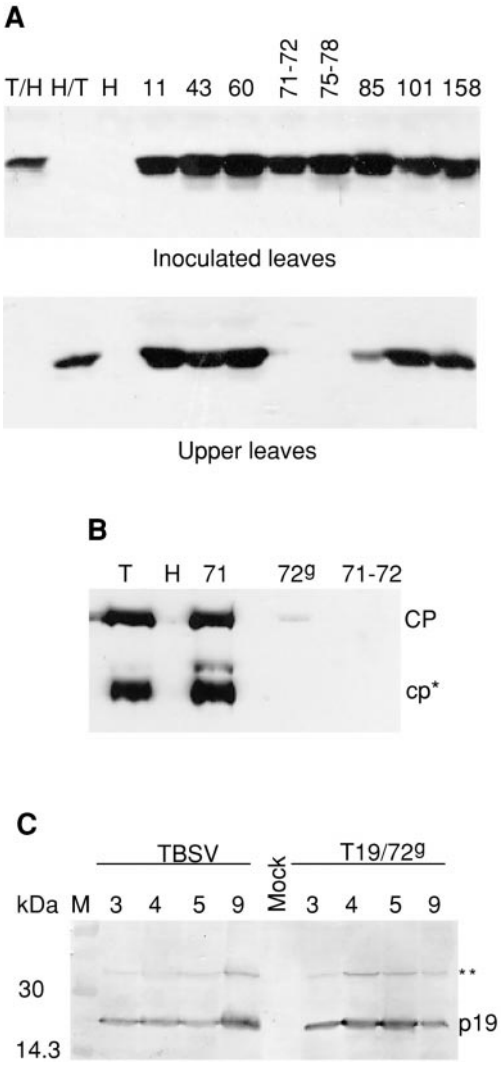

FIG. 4. Effect of p19 mutations on systemic infection of spinach. (A) Inoculated (upper panel) and noninoculated upper (lower panel) leaves were collected from plants 6 or 10 days postinoculation, respectively, with transcripts of mutants whose numerical designations are provided above the lanes. Samples from plants infected with RNA from pTBSV-100 (T) or from healthy plants (H) were used as controls for chemiluminescent immunodetection of the p22-protein. The notation T/H indicates that this lane in the upper panel is T and H in lower panel; H/T in the adjacent lane represents the reciprocal situation. (B) Chemiluminescent immunodetection of the coat protein (CP) in upper noninoculated spinach leaves 8 days after inoculation of lower leaves with transcripts. The migration of a breakdown product of CP is marked by cp*. (C) Alkaline-phosphatase-mediated immunodetection of the p19-protein in extracts from inoculated spinach leaves that were harvested at various days (numbers above lanes) postinoculation with transcripts from either pTBSV-100 (TBSV) or pT19/72[g] (T19/72[g]). Mock inoculated leaves (Mock) were used as control. The molecular weight of protein markers (M) is provided in kDa on the left. The double asterisks indicate the position of presumably dimeric forms of the p19-protein.

at position 72, pT19/71 and pT19/72^{g} were constructed (Fig. 1). For the most part, T19/71 behaved like wild-type TBSV, and rapidly systemically invaded spinach (Fig. 4B). However, infections with T19/72^{g} were mainly limited to inoculated leaves, although some coat protein could be detected by chemiluminescent Western assays in upper leaves (Fig. 4B). As was the case for T19/71–72, systemic infections with T19/72^{g} were notable only when very young spinach plants were inoculated. Time-course studies with inoculated spinach leaves (Fig. 4C) showed that the mutant p19-protein produced by T19/72^{g} accumulated to similar levels in inoculated leaves as the wild-type TBSV p19-protein.

To determine whether the influence of the mutation in pT19/72^{g} was due to a direct effect of arginine substitution, or perhaps to a more indirect structural effect caused by the dramatic change to a glycine, pT19/72^{a} was generated. This mutant produces a p19-protein in which Arg at position 72 was replaced by Ala, which is predicted to have less disturbing influences on the structural integrity than the Gly substitution in pT19/72^{g}. This mutation also caused a substitution of Asp to Leu at position 83 in the p22-protein, but this did not affect cell-to-cell movement. In contrast to what was observed with T19/72^{g}, inoculations of spinach with T19/72^{a} RNA rapidly caused systemic infections in spinach plants (Table 2).

DISCUSSION

Characteristics of p19 mutants

TBSV replication assays in protoplasts failed to detect a direct effect of the p19-protein mutations on accumulation of gRNA and sgRNAs (Fig. 2). This result also signifies that the mutations did not critically influence possible *cis*-acting elements. Such a potential effect was taken into consideration because recent experiments suggest that *cis*-acting sequences reside at the 3′ end of the p19 gene (Park *et al.,* 1998) and in the downstream pX gene (Scholthof and Jackson, 1997), which are sensitive to minor alterations. Immunodetection tests on inoculated *N. benthamiana* and spinach leaves revealed that neither of the introduced mutations noticeably affected cell-to-cell movement based on the accumulation of viral proteins (Figs. 3 and 4). These RNA and protein-accumulation tests confirm earlier observations (Scholthof *et al.,* 1995b) that the TBSV p19-protein is dispensable for replication or cell-to-cell movement in the hosts used in this study. These findings also agree with recent preliminary results that the rate of early replication (occurring between 1–5 h posttransfection) is not influenced by the p19-protein (Qiu *et al.,* 1999). Combined, our data suggest that the p19-protein is not directly involved in replication in protoplasts and that the influence of p19 gene inactivation on accumulation of tombusvirus-defective interfering RNAs (Rochon, 1991), instead may be due to unspecified events in whole plants.

The behavior of the mutant p19-proteins upon SDS–PAGE and subsequent immunoblot assays, was mostly similar to that of wild-type protein, with the exception that the migration of the p19-protein produced by T19/11 was slightly but distinctly retarded (Fig. 3). Perhaps the mutation exerted a conformational effect that was even persistent under denaturing conditions, or it may have influenced putative posttranslational modifications. However, despite this shift in mobility, the p19-protein produced by T19/11 displayed no deviant biological behavior on the hosts used in this study.

In a recent study, we showed that mutants which produced reduced amounts of p19-protein failed to spread in spinach, and the symptoms differed from those induced by the wild-type (Scholthof *et al.,* 1999). Based on these results, a concern was raised for the present study that potential effects of p19 mutations on protein stability could indirectly influence the results. However, immunodetection tests conducted at relatively early time-points using leaves inoculated with p19-mutants, on *N. benthamiana* (Fig. 3) and spinach (Fig. 4C), suggest that relatively high levels of p19-protein were maintained in inoculated leaves up to time points when long-distance systemic invasion was already occurring. Therefore, the observed differences can most likely be attributed directly to the effect of the p19 amino acid substitution(s) on interaction with host (or viral) factors, rather than to potential indirect effects on p19-protein stability.

Biological effects of p19 mutations

The combined results from the biological assays are schematically diagrammed in Table 2, and the salient points will briefly be discussed with regard to the three p19-mediated activities emphasized in this study: (1) induction of a systemic lethal necrosis in *N. benthamiana* or *N. clevelandii*, (2) elicitation of small necrotic local lesions in *N. tabacum,* and (3) the ability of TBSV to spread in spinach. Simultaneous substitution of lysine and arginine at positions 71 and 72 to alanine and glycine (pT19/71–72), or the single replacement of arginine at position 72 to glycine (pT19/72^{g}), or substitution of the two arginine residues at positions 75 and 78 to glycines (pT19/75–78), to various degrees all affect the host-dependent p19-mediated phenotypes. This clustering of domains for these activities differs from our recent results obtained through a similar genetic study on the p22-protein. In that case, essential domains for cell-to-cell movement could genetically be separated from those involved in the elicitation of effective p22-mediated resistance responses (Chu *et al.,* 1999).

Amino acids in the N-terminal region contribute to the elicitation of local lesions on *N. tabacum* or induction of a lethal necrosis on *N. benthamiana* or *N. clevelandii*.

The failure of the p19-proteins produced by pT19/43, pT19/60, and pT19/71–72, to elicit a lethal necrosis in *N. benthamiana* was confirmed upon expression of the individual genes from a PVX vector (data not shown). Similar PVX-mediated expression of wild-type p19-protein induced a systemic collapse of the plants, as previously reported (Scholthof *et al.,* 1995a).

The effect on virus spread in spinach is far more noticeable for the arginine to glycine change at position 72 (pT19/71–72 and pT19/72[g]), compared to the substitution with alanine (pT19/72[a]). This suggests that glycine substitutions may have, as expected, more dramatic effects on protein structure than alanine replacements. However, this conjecture cannot be generalized because glycine substitutions at positions 11, 101, and 158 had no noticeable effect. Therefore, putative indirect effects of glycine substitutions on p19-protein structure are unpredictable and may be position dependent.

Presently, it is not known whether the TBSV p19-protein is actively involved in movement or whether it indirectly assists in virus spread by interfering with defense responses. The multifaceted activities of the p19-protein bear similarities to pathogenicity factors encoded by other viruses, that is, the gene VI protein of caulimoviruses (Schoelz *et al.,* 1991), the 2b gene of cucumber mosaic virus (Ding *et al.,* 1995), or the HC-Pro of potyviruses (Cronin *et al.,* 1995). The recent observation that the HC-Pro may suppress natural defense-related gene silencing events (Anandalakshmi *et al.,* 1998; Brigneti *et al.,* 1998; Kasschau and Carrington, 1998) has prompted the speculation that this may also be a target for virus proteins with similar activities, such as the TBSV p19 protein.

The genetically distinct movement activities of the TBSV p22 and p19 genes resemble the function of the red clover necrotic mosaic (diantho)virus RCNMV movement protein (MP) (Wang *et al.,* 1998). Despite the fact that the cell-to-cell movement function and host-specific long-distance spread are specified by one RCNMV MP, these activities map to distinct regions on this protein. The long-distance spread activity of the RCNMV MP appears to be host-dependent and was shown to involve the passage of cell-type-specific boundaries (Wang *et al.,* 1998). Wild-type TBSV travels from inoculated leaves down to the roots prior to invasion of upper leaves (data not shown), thereby following the classical source/sink pathway discussed by Beijerinck (1999) and shown by Samuel (1934). Considering that T19/71–72 fails to systemically invade spinach (including roots; data not shown), suggests that the wild-type p19-protein may stimulate virus exit from the inoculated spinach leaf in a similar manner as RCNMV MP.

In summary, this study shows that a central region on the p19 polypeptide participates in the onset of local necrotic local lesions in TBSV resistant *N. tabacum*, the induction of a systemic collapse in the p19-independent *N. benthamiana* and *N. clevelandii*, and systemic spread in p19-dependent spinach. However, mutations in the N-terminal region of p19 affected the activities in *Nicotiana* hosts but not in spinach. This implies that the central domain of the p19-protein is either crucial for structural integrity or for direct interaction with host factors involved in spread and symptom induction, whereas the N-terminal portion may be involved in interactions that are more host-specific. This information forms the basis for current biochemical studies on p19-mediated TBSV–plant interactions.

MATERIALS AND METHODS

Bioassays with plants and *N. benthamiana* protoplasts, virus, RNA, or protein analyses were performed as described previously (Scholthof *et al.,* 1993b, 1995b), except that protoplasts were prepared from plants grown in soil in the growth chamber, rather than in Magenta boxes. Standard molecular biology protocols were performed as described by Sambrook *et al.* (1989) or as suggested by suppliers of reagents.

Codons on the p19 gene cDNA specifying charged amino acids were targeted for a PCR-mediated, site-directed mutagenesis, as described previously (Chu *et al.,* 1999). Mutagenic oligonucleotide primers were designed with incorporation of nearby restriction sites (Table 1). Unless otherwise indicated, the 3′ 27-mer primer was used in combination with forward mutagenic primers, whereas "Seq 22A" was used in combination with reverse mutagenic primers (Fig. 1B). Blunt-end PCR fragments were first cloned into the *Sma*I site of pKAN2 (Scholthof *et al.,* 1995a), prior to transfer into pTBSV-100, an infectious full-length cDNA clone of the cherry strain of TBSV (Hearne *et al.,* 1990), using strategies outlined for each construct discussed below. The authenticity of mutations was confirmed by sequence analysis.

To generate pT19/11, the *Nco*I–*Sal*I fragment (nt 3885–4499) from the pKAN2 intermediate was used to replace the corresponding region of pHS136 (Scholthof *et al.,* 1995b). The latter plasmid is a full-length cDNA clone with an inactive p22 gene through the introduction of a mutation that had introduced an *Avr*II site. This feature facilitated screening of recombinants because successful replacement with the region carrying the T19/11 mutation resulted in a construct devoid of this *Avr*II site. For construction of pT19/43, a *Pfl*MI–*Eco*RI fragment (nt 3848–4033) from the pKAN2 intermediate was cloned into pHS11, in which the *Nco*I site at position 3885 was removed (Scholthof *et al.,* 1995b). Restoration of the *Nco*I site was used as the criterion for screening of the full-length TBSV cDNA containing the fragment with the desired mutation. The plasmid pT19/60 contains an *Eco*RI–*Sma*I fragment (nt 4033–4773) from the pKAN2 intermediate, that was inserted into pHS10–13, in which a *Sal*I site was absent (Scholthof and Jackson, 1997).

To obtain pT19/71–72, an extra cloning step was necessary because the *Eco*RV site used to introduce the nearby mutation is not unique in the full-length cDNA clone. For this purpose, the *Pfl*MI–*Eco*RV fragment (nt 3848–4101) containing the mutations was first cloned into pHS49, a subclone of pTBSV-100 (Scholthof and Jackson, 1997). Subsequently the *Pfl*MI–*Sal*I fragment with the mutations was used to replace the corresponding fragment of pHS11. To incorporate mutations into pT19/71 and pT19/72^{g}, the PCR fragments harboring these mutations were cloned into pKAN157Δ*Eco*RV. This intermediate contains the *Bam*HI to *Sph*I fragment of pHS157 (Scholthof *et al.,* 1995b), cloned into pKAN2, from which an internal *Eco*RV fragment was subsequently removed. The mutant PCR fragments were digested with *Eco*RV and cloned into pKAN157Δ*Eco*RV, linearized with *Eco*RV. The *Pfl*MI–*Hpa*I fragments from these resulting constructs were then cloned into pHS11 to obtain pT19/71 and pT19/72^{g}, respectively.

To obtain pT19/75–78, the primer Amber-seq was used as the forward primer (Fig. 1B), followed by cloning of the PCR fragment into pKAN2. Subsequently, the *Hin*dIII fragment (nt 2373–4125) of this intermediate was used to replace the corresponding fragment of the DNA-based TBSV gene vector pHST12 (Scholthof, 1999). The resulting plasmid (pD20/75–78), was infectious by rub-inoculation of the DNA onto plants (data not shown). To eliminate the possibility that phenotypic differences could possibly be influenced by using DNA inoculum instead of *in vitro* generated transcripts, the *Pfl*MI–*Sal*I fragment (nt 3848–4499) of pD20/75–78 was used to substitute the corresponding fragment of pHS11, to yield pT19/75–78, from which transcripts could be generated.

Two steps were involved in making pT19/85. First, the cloned PCR fragment in pKAN2 was digested with *Hin*dIII and *Sal*I, and this fragment was used to replace the analogous segment in a construct derived from pHST12, in which the *Stu*I–*Bam*HI (nt 1058–2439) region was deleted, leaving a unique *Hin*dIII site at position 4125. Second, the *Pfl*MI–*Sal*I fragment from this intermediate clone was used to substitute the corresponding fragment of pHS11 to yield pT19/85. To obtain pT19/101, the *Hpa*I–*Sph*I fragment (nt 4169–4775) from the pKAN2 intermediate was used to replace the corresponding fragment of pHS10–13, in which the *Sal*I site at position 4499 is eliminated (Scholthof and Jackson, 1997). Construction of pT19/157 involved a two-step procedure. A *Bst*BI fragment (nt 4036–4385) from the PCR product was used to replace the corresponding fragment of pHS49. Subsequently, the *Pfl*MI–*Sal*I fragment from this intermediate construct was used to substitute the analogous fragment of pHS11.

The mutations in pT19/72^{a} and pT19/104 were introduced using the oligonucleotide site-directed mutagenesis procedure (Sambrook *et al.,* 1989). The single-stranded DNA template for this mutagenesis was derived from a pBS plasmid containing the *Not*I to *Sal*I fragment of pTBSV-100. The *Pfl*MI to *Sal*I fragments carrying the mutations were then used to replace the corresponding fragment of pHS57 (Scholthof *et al.,* 1995b).

ACKNOWLEDGMENTS

We are grateful to Joan Kuecker and Beth Whitehead for supplying plant material used in these experiments, and to Karen-Beth G. Scholthof, Wenping Qiu, and Jong-Won Park for very valuable suggestions during the experiments and the preparation of the manuscript. This work was funded by grants from USDA/CSREES-NRI-CGP (95-37303-2289) and the Texas Higher Education Coordinating Board Advanced Research Program (999902-056).

REFERENCES

Anandalakshmi, R., Pruss, G. J., Ge, X., Marathe, R., Mallory, A. C., Smith, T. H., and Vance, V. B. (1998). A viral suppressor of gene silencing in plants. *Proc. Natl. Acad. Sci. USA* **95,** 13079–13084.

Beijerinck, M. W. (1999). Concerning a contagium vivum fluidum as cause of the spot disease of tobacco leaves. *In* "Tobacco Mosaic Virus: One Hundred Years of Contributions to Virology" (K.-B. G. Scholthof, J. G. Shaw, and M. Zaitlin, Eds.). American Phytopathological Society Press, St. Paul, MN.

Brigneti, G., Voinnet, O., Li, W.-X., Ji, L.-H., Ding, S. W., and Baulcombe, D. C. (1998). Viral pathogenecity determinants are suppressors of transgene silencing in *Nicotiana benthamiana. EMBO J.* **17,** 6739–6746.

Chu, M., Park, J.-W., and Scholthof, H. B. (1999). Separate regions on the tomato bushy stunt virus p22 protein mediate cell-to-cell movement versus elicitation of effective resistance responses. *Mol. Plant Microbe Interact.* **12,** 285–292.

Cronin, S., Verchot, J., Haldeman-Cahill, R., Schaad, M. C., and Carrington, J. C. (1995). Long-distance movement factor: a transport function of the potyvirus helper component-proteinase. *Plant Cell* **7,** 549–559.

Dalmay, T., Rubino, L., Burgyan, J., Kollar, A., and Russo, M. (1993). Functional analysis of cymbidium ringspot virus genome. *Virology* **194,** 697–704.

Ding, S. W., Li, W.-X., and Symons, R. H. (1995). A novel naturally occurring hybrid gene encoded by a plant virus RNA facilitates long distance virus movement. *EMBO J.* **14,** 5762–5772.

Havelda, Z., Szittya, G., and Burgyan, J. (1998). Characterization of the molecular mechanism of defective interfering RNA-mediated symptom attenuation in tombusvirus-infected plants. *J. Virol.* **72,** 6251–6256.

Hayes, R. J., Brunt, A. A., and Buck, K. W. (1988). Gene mapping and expression of tomato bushy stunt virus. *J. Gen. Virol.* **69,** 3047–3057.

Hearne, P. Q., Knorr, D. A., Hillman, B. I., and Morris, T. J. (1990). The complete genome structure and synthesis of infectious RNA from clones of tomato bushy stunt virus. *Virology* **177,** 141–151.

Hillman, B. I., Hearne, P., Rochon, D. A., and Morris, T. J. (1989). Organization of tomato bushy stunt virus genome: characterization of the coat protein gene and the 3′ terminus. *Virology* **169,** 42–50.

Johnston, J. C., and Rochon, D. M. (1995). Deletion analysis of the promoter for the cucumber necrosis virus 0.9-kb subgenomic RNA. *Virology* **214,** 100–109.

Johnston, J. C., and Rochon, D. M. (1996). Both codon context and leader length contribute to efficient expression of two overlapping open reading frames of a cucumber necrosis virus bifunctional subgenomic mRNA. *Virology* **221,** 232–239.

Kasschau, K. D., and Carrington, J. C. (1998). A counterdefensive strategy of plant viruses: suppression of posttranscriptional gene silencing. *Cell* **95,** 461–470.

Martelli, G. P., Gallitelli, D., and Russo, M. (1988). Tombusviruses. *In*

"The Plant Viruses" (R. Koenig, Ed.), Vol. 3, pp. 13–72. Plenum, New York.

Park, J.-W., Qiu, W. P., Desvoyes, B., and Scholthof, H. B. (1998). Accumulation of tomato bushy stunt virus is influenced by host-specific cis-acting RNA elements. *Phytopathology* **88,** S70. [Abstract]

Qiu, W. P., Park, J.-W., and Scholthof, H. B. (1999). Analysis of viral factors affecting accumulation of tomato bushy stunt virus RNAs. *Phytopathology* **89,** S62 (Abstract).

Reade, R., Wu, Z., and Rochon, D. (1999). Both RNA rearrangement and point mutation contribute to repair of defective chimeric viral genomes to form functional hybrid viruses in plants. *Virology* **258,** 217–231.

Rochon, D. M. (1991). Rapid *de novo* generation of defective interfering RNA by cucumber necrosis mutants that do not express the 20-kDa nonstructural protein. *Proc. Natl. Acad. Sci. USA* **88,** 11153–11157.

Russo, M., Burgyan, J., and Martelli, G. P. (1994). Molecular biology of Tombusviridae. *Adv. Virus Res.* **44,** 381–428.

Sambrook, J., Fritsch, E. F., and Maniatis, T. (1989). "Molecular Cloning: A Laboratory Manual, 2nd ed." Cold Spring Harbor Laboratory Press, Cold Spring Harbor, NY.

Samuel, G. (1934). The movement of tobacco mosaic virus within the plant. *Ann. Appl. Biol.* **21,** 90–111.

Schoelz, J. E., Goldberg, K.-B., and Kiernan, J. (1991). Expression of cauliflower mosaic virus (CaMV) gene VI in transgenic *Nicotiana bigelovii* complements a strain of CaMV defective in long-distance movement in nontransformed *N. bigelovii. Mol. Plant Microbe Interact.* **4,** 350–355.

Scholthof, H. B. (1999). Rapid delivery of foreign genes into plants by direct rub-inoculation with intact plasmid DNA of a tomato bushy stunt virus gene vector. *J. Virol.* **73,** 7823–7829.

Scholthof, H. B., Borja, M., Morris, T. J., and Jackson, A. O. (1993a). Molecular approaches for control of tomato bushy stunt virus. *In* "Molecular Biology of Tomato: Fundamental Advances and Crop Improvement" (J. I. Yoder, Ed.), pp. 239–249. Technomic Publishing, Lancaster, PA.

Scholthof, H. B., Desvoyes, B., Kuecker, J., and Whitehead, E. (1999). The biological activity of two tombus virus proteins translated from nested genes is influenced by dosage control via context-dependent leaky scanning. *Mol. Plant Microbe Interact.* **12,** 670–679.

Scholthof, H. B., and Jackson, A. O. (1997). The enigma of pX: a host dependent cis-acting element with variable effects on tombusvirus RNA accumulation. *Virology* **237,** 56–65.

Scholthof, H. B., Morris, T. J., and Jackson, A. O. (1993b). The capsid protein gene of tomato bushy stunt virus is dispensable for systemic movement and can be replaced for localized expression of foreign genes. *Mol. Plant Microbe Interact.* **6,** 309–322.

Scholthof, H. B., Scholthof, K.-B. G., and Jackson, A. O. (1995a). Identification of tomato bushy stunt virus host-specific symptom determinants by expression of individual genes from a potato virus X vector. *Plant Cell* **7,** 1157–1172.

Scholthof, H. B., Scholthof, K.-B. G., Kikkert, M., and Jackson, A. O. (1995b). Tomato bushy stunt virus spread is regulated by two nested genes that function in cell-to-cell movement and host-dependent systemic invasion. *Virology* **213,** 425–438.

Scholthof, K.-B. G., Scholthof, H. B., and Jackson, A. O. (1995c). The tomato bushy stunt virus replicase proteins are coordinately expressed and membrane associated. *Virology* **208,** 365–369.

Wang, H.-L., Wang, Y., Giesman-Cookmeyer, D., Lommel, S. A., and Lucas, W. J. (1998). Mutations in viral movement protein alter systemic infection and identify an intercellular barrier to entry into the phloem long-distance transport system. *Virology* **245,** 75–89.

Zhang, G., Slowinski, V., and White, K. A. (1999). Subgenomic mRNA regulation by a distal RNA element in a (+)strand RNA virus. *RNA* **5,** 550–561.